

MIT Open Access Articles

Global Analysis of Macular Choriocapillaris Perfusion in Dry Age-Related Macular Degeneration using Swept-Source Optical Coherence Tomography Angiography

The MIT Faculty has made this article openly available. **Please share** how this access benefits you. Your story matters.

Citation: Braun, Phillip X. et al. "Global Analysis of Macular Choriocapillaris Perfusion in Dry Age-Related Macular Degeneration using Swept-Source Optical Coherence Tomography Angiography." *Investigative Ophthalmology and Visual Science* 60, 15 (December 2019): 4985–4990. © 2019 The Authors

As Published: <http://dx.doi.org/10.1167/iovs.19-27861>

Publisher: Association for Research in Vision and Ophthalmology (ARVO)

Persistent URL: <https://hdl.handle.net/1721.1/128928>

Version: Final published version: final published article, as it appeared in a journal, conference proceedings, or other formally published context

Terms of use: Creative Commons Attribution-NonCommercial-NoDerivs License



Global Analysis of Macular Choriocapillaris Perfusion in Dry Age-Related Macular Degeneration using Swept-Source Optical Coherence Tomography Angiography

Phillip X. Braun,^{1,2} Nihaal Mehta,^{1,3} Isaac Gendelman,^{1,4} A. Yasin Alibhai,¹ Eric M. Moulton,⁵ Yi Zhao,⁶ Akihiro Ishibazawa,^{1,7} Osama Sorour,^{1,8} Eleni K. Konstantinou,¹ Caroline R. Baumal,¹ Andre J. Witkin,¹ James G. Fujimoto,⁵ Jay S. Duker,¹ and Nadia K. Waheed¹

¹New England Eye Center, Tufts Medical Center, Boston, Massachusetts, United States

²Yale University School of Medicine, New Haven, Connecticut, United States

³Warren Alpert Medical School of Brown University, Providence, Rhode Island, United States

⁴Tufts University School of Medicine, Boston, Massachusetts, United States

⁵Department of Electrical Engineering and Computer Science, Massachusetts Institute of Technology, Cambridge, Massachusetts, United States

⁶Friedman School of Nutrition Science and Policy, Tufts University, Boston, Massachusetts, United States

⁷Department of Ophthalmology, Asahikawa Medical University, Asahikawa, Japan

⁸Department of Ophthalmology, Tanta University, Tanta, Egypt

Correspondence: Nadia K. Waheed, New England Eye Center, 260 Tremont Street, Boston, MA 02116, USA; nadiakwaheed@gmail.com.

Submitted: June 29, 2019

Accepted: October 19, 2019

Citation: Braun PX, Mehta N, Gendelman I, et al. Global analysis of macular choriocapillaris perfusion in dry age-related macular degeneration using swept-source optical coherence tomography angiography. *Invest Ophthalmol Vis Sci.* 2019;60:4985–4990. <https://doi.org/10.1167/iovs.19-27861>

PURPOSE. Swept-source optical coherence tomography angiography (SS-OCTA) was used to investigate if the clinical stage of dry age-related macular degeneration (AMD) was correlated with global and regional macular choriocapillaris (CC) perfusion.

METHODS. In this retrospective, cross-sectional study, 6×6 -mm SS-OCTA images from eyes with early, intermediate, and advanced dry AMD (56 eyes, 41 patients) were analyzed using algorithms described in the literature to assess regional flow deficit percentage (FD%) and average flow deficit size. Regions were defined by concentric areas centered on the fovea: a 1-mm-diameter area, 3-mm-diameter ring, 5-mm-diameter area, 5-mm-diameter ring, and 6×6 -mm whole image. Data were modeled using the generalized estimating equations approach.

RESULTS. The relationship between age and CC FD% and average flow deficit size was statistically significant ($P \leq 0.05$) in all regions of analysis by linear modeling. The relationship between dry AMD stage and FD% was statistically significant by linear modeling in the 5-mm ring, and between dry AMD stage and average flow deficit size in the 3-mm ring, 5-mm area, 5-mm ring, and 6×6 -mm whole image.

CONCLUSIONS. Linear modeling suggests a statistically significant relationship between dry AMD stage and CC perfusion, most prominent in the more peripheral regions of the macula.

Keywords: OCTA, macula, choriocapillaris, retina, dry age-related macular degeneration

Age-related macular degeneration (AMD) is a leading cause of permanent visual loss worldwide.¹ A major breakthrough in addressing this disease was the introduction of anti-VEGF therapy, which enabled substantially improved vision in patients with wet (neovascular) AMD.² However, there are currently no proven therapeutic options for patients with dry (non-neovascular) AMD.³ A major reason that dry AMD is attractive as a therapeutic target is that, in its earlier stages, patient vision is generally much better preserved than in its more advanced forms, which include geographic atrophy (GA) and conversion to wet AMD.^{1,4} However, to develop potential interventions, the pathophysiology of dry AMD must be better understood.^{1,5} Working toward this understanding has been a matter of great interest, particularly of late.^{3,4,6,7}

One line of inquiry with respect to the etiology of dry AMD concerns the role of the choriocapillaris (CC).⁶ The CC interfaces with the retinal pigment epithelium (RPE) and the photoreceptors through Bruch's membrane, supplying metabolic needs and removing metabolic wastes. In dry AMD, this

association is frequently altered, as when drusen separate RPE from Bruch's membrane, or when there is CC loss. It is known that the CC is impaired in both structure and flow in the various stages of dry AMD.^{1,6,8–11} Histological studies demonstrate impairment in CC structure in various stages of dry AMD, but it is not clear whether CC loss precedes, follows, or develops simultaneously with RPE loss, a determination that may have implications for causality.^{9,12–14} The limitations of histological inquiry include restriction to postmortem examination and often small sample sizes. Digital fluorescein angiography is unsuitable for CC investigation, as it is not depth resolved and practical applications are limited to the superficial retinal vascular plexus. Indocyanine green angiography, although able to visualize CC circulation, also suffers from a lack of depth resolution and therefore cannot distinguish CC flow from deeper choroidal flow.^{5,15}

Optical coherence tomography (OCT) angiography (OCTA), although facing its own limitations including a restriction to measurement of blood flow as opposed to structure, as well as



limits on measurable speed of flow,^{5,10} offers a number of unique advantages to investigation of the CC. OCTA is currently the only modality that offers rapid, noninvasive, depth-resolved, in vivo imaging of CC flow,^{5,6,9,10,15} features that lend great promise for both research and clinical applications. For example, it has been suggested that CC flow deficits may correlate with rate of AMD progression, thereby highlighting the potential of OCTA for risk stratification in clinical trials and possible future interventions.^{16,17} Its potential for CC investigation has been enhanced with the use of longer-wavelength light sources, which enables superior signal penetration through the highly scattering RPE, a particularly important feature for visualizing the CC beneath additional attenuating structures such as drusen.^{5,10,18–21}

There have been a number of investigations of the CC in dry AMD using OCTA. Findings have included increased flow deficits in early and intermediate dry AMD versus age-matched controls, with further focal deficits⁶; flow deficits concentrated beneath drusen using swept-source (SS)-OCTA and peri-drusen areas using both spectral domain (SD-) and SS-OCTA^{8,22}; and loss of CC beneath GA lesions and to a lesser extent in areas surrounding these lesions.^{15,19,23} Recently, Sacconi et al.,²⁴ Nassisi et al.,²⁵ and Zheng et al.²⁶ used commercially available SS-OCTA to characterize global flow characteristics of the macular CC in healthy patients. All groups found a decrease in CC perfusion associated with advancing age that preferentially affected the central macula. The current study endeavors to characterize more fully the macular CC in dry AMD, taking into consideration this improved understanding of the correlation of age with macular CC in normal eyes. In particular, the central questions of this study are (1) whether dry AMD stage has a relationship with macular CC perfusion, and (2) how this relationship (if any) varies by region.

METHODS

This retrospective, cross-sectional study requiring informed consent was approved by the Institutional Review Board of Tufts Medical Center and adhered to the requirements of the Declaration of Helsinki and the Health Insurance Portability and Accountability Act. All patients who had been diagnosed clinically with dry AMD in at least one eye by a retinal specialist and were recorded in a database as having been imaged on an SS-OCTA instrument (PLEX Elite 9000; Carl Zeiss Meditec, Dublin, CA, USA) from December 2016 to September 2018 were considered for the study. Fellow eyes in patients with a diagnosis of wet AMD were eligible for inclusion; eyes with quiescent macular neovascularization were not. Exclusion criteria consisted of the following: poor-quality images (e.g., affected by motion artifact); retinal diagnoses or other pathologies that could potentially affect the CC (e.g., diabetes mellitus, glaucoma), excepting epiretinal membrane, history of retinal hole, tear, or schisis, and choroidal nevus; eyes lacking imaging, within 9 months of their OCTA image, on an OCT instrument (Cirrus 5000 HD-OCT; Carl Zeiss Meditec) whose software was used to stage their dry AMD; images having an OCTA signal strength of 5/10 or lower (three 6/10 images visually inspected for quality were included, with all other images 7/10 or higher); and myopia^{5,8} greater than -3.5 diopters.

Patients were subsequently staged according to the following dry AMD criteria²⁷: advanced eyes had GA or nascent GA as defined by hypertransmissive lesions greater than or equal to 125 μm along their greatest linear dimension on en face OCT imaging, a size that was confirmed on OCT B-scan; intermediate eyes were characterized by a drusen volume greater than or equal to 0.02 mm^3 within a 3-mm-diameter

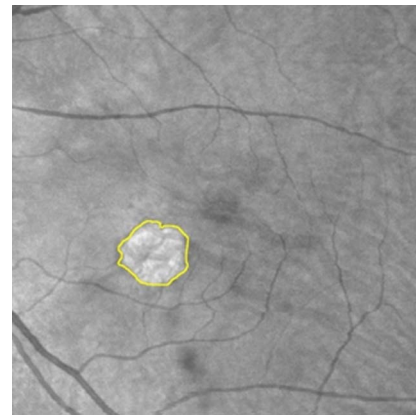


FIGURE 1. Exclusion of GA lesions in advanced patients. PLEX Elite “Whole Eye” structural images were scaled appropriately, then, after validation of complete RPE loss on OCT B-scan, used to create masks that were applied to their angiographic correlates at the level of the CC. These regions were then excluded from concentric circular and whole image analysis for flow deficit metrics.

circle centered on the fovea, and did not meet criteria for advanced classification; eyes with a drusen volume less than 0.02 mm^3 within a 3-mm-diameter circle centered on the fovea, and that did not meet criteria for advanced classification, were categorized as early stage.

The PLEX Elite 9000 has an A-scan rate of 100,000 scans per second, a central wavelength of 1060 nm, an axial resolution of approximately 6 μm in tissue, a lateral resolution of approximately 14 μm at the retinal surface, and images at a depth of 3 mm. The macula-centered 6 \times 6-mm en face images used in this study are composed of 500 B-scans at 500 A-scans per B-scan. As in prior studies of the CC,^{17,20} segmentation of the CC slab in all eyes involved maximum projection 20 μm deep to Bruch’s membrane. For early eyes, the instrument’s “RPEfit” segmentation algorithm was used, with manual adjustment as needed; intermediate and advanced eyes were manually segmented due to numerous drusen and RPE distortions. In addition, regions of GA (total RPE loss) in the advanced group were excluded from analysis as described in Figure 1. All manual segmentation and exclusion of GA were performed with a precision drawing tablet (Intuos; Wacom, Portland, OR, USA). Superficial vascular projections were addressed using the PLEX Elite software’s projection removal algorithm before image export.^{16,19} Exported images were processed using an algorithm written in ImageJ, version 1.52h (<http://imagej.nih.gov/ij/>; provided in the public domain by the National Institutes of Health, Bethesda, MD, USA) based on a previously described formula to compensate for signal attenuation beneath drusen.^{19,20,26} Because of this compensation algorithm, only regions of complete signal loss on both the angiography en face image and its structural correlate were excluded from analysis, as were any areas of significant structural artifact.⁵ Images were subsequently binarized using a Phansalkar local threshold (radius: 15 px)^{16,25} and inverted to highlight flow deficits. The “Analyze Particles” command (size: 1-Infinity; circularity 0–1) was then run on five different regions of analysis for each image, as described in Figure 2. Flow deficit metrics included flow deficit percentage (FD%) and average flow deficit size. In advanced eyes, regions of analysis with GA exclusions resulting in total flow deficit areas of 500 px^2 or less were excluded. This is approximately equivalent to the size of a single large druse in 6 \times 6-mm images or 0.05% of total 6 \times 6-mm area. This was done to minimize weighting flow deficit metrics in miniscule areas equally with

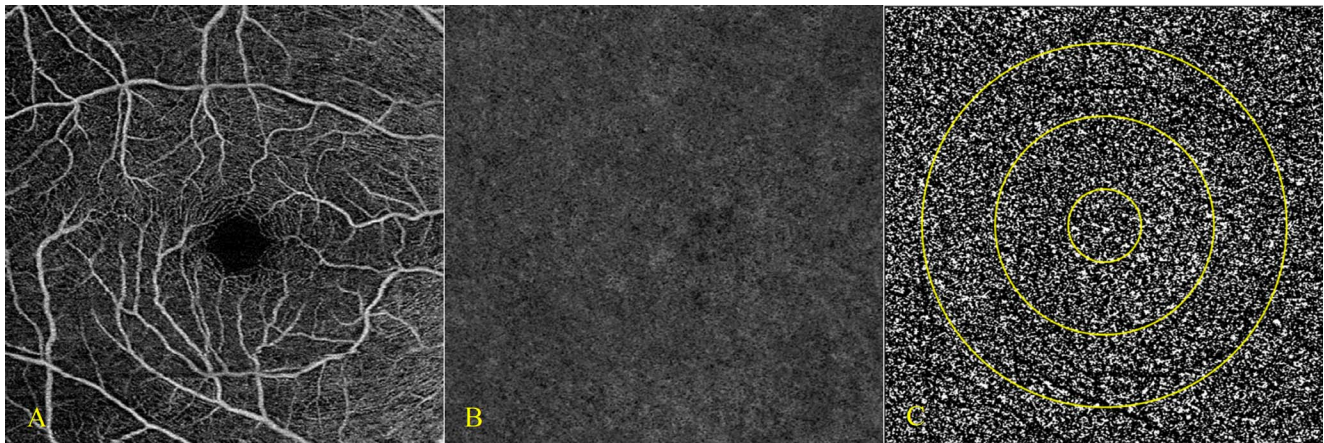


FIGURE 2. (A) OCTA image of eye with early dry AMD at the level of the superficial capillary plexus. (B) Original OCTA image at the level of the CC. (C) Image after signal attenuation compensation, binarization, and inversion to show deficits rather than flow in *white*, overlaid with *circular regions of analysis* within which particle analysis was conducted. Regions of analysis: a 1-mm-diameter area centered on the fovea, a 3-mm-diameter ring (exclusive of 1-mm-diameter central area), a 5-mm-diameter area centered on the fovea, a 5-mm-diameter ring (exclusive of 3-mm-diameter central area), and whole 6×6 -mm image.

much larger (often at least an order of magnitude) corresponding regions of analysis in other images.

Statistically, the object was to discern what, if any, relationship dry AMD stage had to each of the two flow deficit metrics in each of the regions of analysis. To discern the independent contributions by age, stage, and eye side (OD or OS) to FD% and average flow deficit size, the generalized estimating equations (GEE) method was used. This approach to linear modeling has particular utility for ophthalmology studies, as it can account for the correlation between fellow eyes.²⁸ All dry AMD stages were included in a single linear model for each flow deficit metric at each region of analysis (10 models total), with each model incorporating age and eye side as covariates. A *P* value of 0.05 was used to determine statistical significance. Statistical analysis was performed using JMP Pro (version 13.2.1; SAS Institute Inc., Cary, NC, USA) and R (R Foundation for Statistical Computing, Vienna, Austria).

RESULTS

A total of 56 eyes from 41 patients were included in this study. Staging resulted in 23 early, 12 intermediate, and 21 advanced eyes (detailed characteristics in Table 1.) Before application of the 500 px² total flow deficit area threshold to advanced eyes, because of GA entirely consuming regions in some images there were 18, 20, 21, 21, and 21 6×6 mm images available for the 1-mm area, 3-mm ring, 5-mm area, 5-mm ring, and whole image regions of analysis, respectively. After applying this 500 px² threshold there were 16, 19, 21, 21, and 21 6×6 mm images available for the 1-mm area, 3-mm ring, 5-mm area, 5-mm ring, and whole image regions of analysis, respectively.

TABLE 1. Study Patient and Eye Characteristics Stratified by Dry AMD Stage

Stage	Patients				Eyes				
	Age, Mean (SD) [Range]	Sex		Age, Mean (SD) [Range]	Sex		Side		
		M	F		M	F	OD	OS	
Early	73 (6.1) [60–85]	4	12	72 (6.3) [60–85]	5	18	14	9	
Intermediate	80 (8.9) [63–88]	4	4	77 (9.9) [63–88]	7	5	5	7	
Advanced	81 (7.2) [69–97]	5	12	81 (7.4) [69–97]	8	13	7	14	
All patients	78 (8.0) [60–97]	13	28	77 (8.6) [60–97]	20	36	26	30	

Summary statistics for each dry AMD stage and each region of analysis are shown in Table 2, with example images of flow deficits at each stage and region shown in Figure 3. Mean flow deficit metrics increase with disease stage progression, with the exception of mean average flow deficit size in the 5-mm area, 5-mm ring, and whole image. Standard deviations increase with disease stage progression for both flow deficit metrics. For all stages of dry AMD, flow deficit metrics tend to decrease with increased distance from the central macula.

On GEE analysis (Table 3), the relationship between age and both flow deficit metrics was significant in all regions of analysis. Peripheral regions most consistently demonstrated a significant relationship between stage and both flow deficit metrics: FD% $P \leq 0.05$ in the 5-mm ring region of analysis, and average flow deficit size $P \leq 0.05$ in the 3-mm ring, 5-mm area, 5-mm ring, and whole image regions of analysis. There was no significant relationship between eye side and flow deficit metrics in any region of analysis.

DISCUSSION

Previous OCTA studies of the CC in dry AMD have focused on individual lesions and their surrounding areas,^{15,16,19,21} with some limited work on global analysis and staging.^{6,8,22} This study endeavored to investigate the CC quantitatively throughout the macula in all stages of dry AMD. GA lesions were themselves excluded from analysis because these areas are known to have extensive and often complete underlying CC loss,^{5,12} as well as morphological changes resulting in effective flow reduction like reduced branching and severe constriction,^{9,13} which could inappropriately skew quantification and

TABLE 2. Summary Statistics for All Dry AMD Stages and Regions of Analysis

	FD%			Average Flow Deficit Size (μm^2)		
	Early	Intermediate	Advanced	Early	Intermediate	Advanced
1-mm area						
Mean (SD)	26.9 (3.2)	31.7 (7.4)	33.9 (8.0)	710.7 (230.0)	944.1 (593.9)	1349.2 (834.3)
[Range]	[22.0-35.5]	[23.9-45.0]	[20.0-46.6]	[381.1-1407.6]	[418.9-2053.1]	[326.2-3457.2]
3-mm ring						
Mean (SD)	26.4 (3.2)	29.8 (5.7)	36.6 (11.6)	700.4 (219.7)	796.5 (394.8)	1479.7 (1023.1)
[Range]	[22.1-32.7]	[22.5-38.6]	[18.7-58.1]	[370.8-1119.2]	[377.7-1606.7]	[315.9-3701.0]
5-mm area						
Mean (SD)	25.6 (2.8)	27.3 (4.4)	32.1 (7.4)	676.3 (192.3)	672.9 (291.8)	1239.4 (748.4)
[Range]	[20.7-31.8]	[20.8-34.2]	[18.4-43.4]	[384.5-1054.0]	[353.6-1263.4]	[309.0-2763.7]
5-mm ring						
Mean (SD)	25.3 (2.9)	25.8 (3.8)	31.4 (7.4)	655.7 (192.3)	587.1 (240.3)	1157.0 (676.3)
[Range]	[19.7-31.3]	[19.6-32.1]	[18.2-43.0]	[381.1-1005.9]	[329.6-1060.9]	[298.7-2396.4]
Whole image						
Mean (SD)	25.2 (2.9)	25.9 (3.8)	30.1 (6.4)	669.5 (192.3)	604.2 (247.2)	1050.6 (535.6)
[Range]	[19.5-31.9]	[19.5-31.8]	[18.6-39.2]	[394.8-1084.9]	[336.5-1091.8]	[315.9-2087.4]

thus mask the effect of subtler pathological CC changes (e.g., in nascent GA, drusen-associated GA, and peri-GA areas). GA lesion exclusion was also important to minimize detection of choroidal flow, because larger choroidal vessels tend to move inward to occupy CC space when the CC has been lost.^{5,6}

To address the central questions posed by this study, results (1) reaffirm the conclusion of previous studies that age has a strong correlation with flow deficit metrics in the macular CC, and (2) suggest that there is a relationship between dry AMD stage and CC perfusion by linear modeling, more pronounced with increased distance from the fovea. The age-flow deficit correlation was first shown on OCTA by Alten et al.²⁹ and Spaide,³⁰ which agreed with histological findings.^{9,31} Sacconi et al.,²⁴ Nassisi et al.,²⁵ and Zheng et al.²⁶ used OCTA to further specify regional differences in this correlation through topographic analyses. These three studies suggest one possible interpretation of the current study's results, namely, that a strong effect of age on the CC toward the center of the macula may mask any dry AMD stage effects in this area, whereas toward the macular periphery, where age seems to have a reduced influence on the CC, the effects of stage become more distinguishable. Alternatively, AMD may indeed cause earlier CC alterations outside the foveal region and this may contribute to the propensity of GA to begin extrafoveally,³²

but it is clearly beyond the scope of this cross-sectional study to answer such questions. From a histological perspective, although a corresponding study of macular topography has not been performed, results of the current study seem consistent with the findings of Seddon et al.,⁹ who found CC attenuation with advancing dry AMD stage, particularly from the intermediate to the advanced (GA) stage.

It is important to note the difficulties of segmentation in OCTA studies of the CC when the RPE is distorted, as in more advanced dry AMD. Autosegmentation algorithms are currently inadequate. Irregular RPE thickening and drusen both can make segmentation of Bruch's membrane a task that requires great care. Every aid to accurate segmentation is appropriate, from use of a drawing tablet to the ability to adjust OCT B-scan contrast for Bruch's membrane identification. Commercial developments, including improved autosegmentation algorithms and higher axial resolution, could go some way toward enhancing CC investigation in eyes with diseased RPE. Because of the challenging nature of CC investigation using OCTA in the setting of dry AMD in particular, caution must be exercised in drawing pathophysiologic conclusions. However, in the current study, careful methodology and points of accord with known CC structure and function are encouraging toward this end.

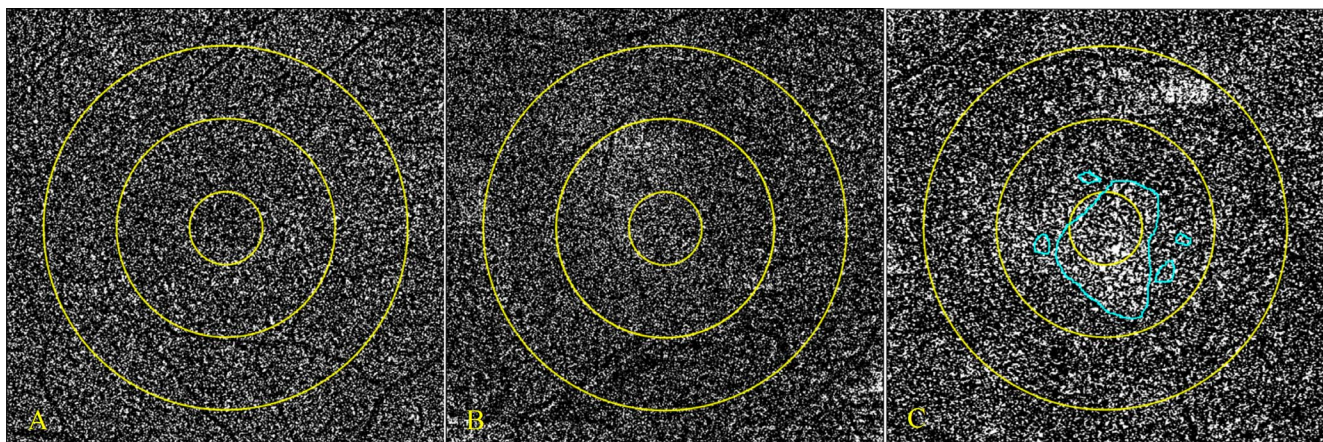


FIGURE 3. Binarized and inverted images (CC flow deficits in white) of eyes with early (A), intermediate (B), and advanced (C) dry AMD, overlaid with regions of analysis. The blue outline in (C) represents areas of GA, which were excluded from analysis.

TABLE 3. P Values of Model Terms (Linear Regression Coefficients for Age, Eye Side, Stage) for All Regions of Analysis

	FD%				Average Size			
	Age	Side	Interstage Comparison	Stage	Age	Side	Interstage Comparison	Stage
1-mm area	0.008 †	0.854	Early vs. intermediate	0.140	0.005 †	0.537	Early vs. intermediate	0.722
			Early vs. advanced	0.170			Early vs. advanced	0.162
			Intermediate vs. advanced	0.903			Intermediate vs. advanced	0.365
3-mm ring	0.002 †	0.825	Early vs. intermediate	0.484	0.005 †	0.060	Early vs. intermediate	0.283
			Early vs. advanced	0.054			Early vs. advanced	0.102
			Intermediate vs. advanced	0.115			Intermediate vs. advanced	0.036 *
5-mm area	1E-5 ‡	0.951	Early vs. intermediate	0.661	3E-4 ‡	0.266	Early vs. intermediate	0.060
			Early vs. advanced	0.120			Early vs. advanced	0.110
			Intermediate vs. advanced	0.064			Intermediate vs. advanced	0.007 †
5-mm ring	2E-5 ‡	0.976	Early vs. intermediate	0.177	8E-5 ‡	0.438	Early vs. intermediate	0.015 *
			Early vs. advanced	0.170			Early vs. advanced	0.135
			Intermediate vs. advanced	0.016 *			Intermediate vs. advanced	0.002 †
Whole image	3E-7 ‡	0.433	Early vs. intermediate	0.248	3E-5 ‡	0.805	Early vs. intermediate	0.013 *
			Early vs. advanced	0.280			Early vs. advanced	0.231
			Intermediate vs. advanced	0.056			Intermediate vs. advanced	0.005 †

Boldface indicates statistical significance defined as $P \leq 0.05$. Side is eye side (OD versus OS comparison).

* $P \leq 0.05$.

† $P \leq 0.01$.

‡ $P \leq 0.001$.

Although there has been discussion about the extent to which reticular pseudodrusen (RPD) reflect CC flow impairment relative to true drusen,^{33,34} it did not seem unreasonable to include eyes with RPD in the study cohort. Because previous work^{35,36} suggests that RPD prevalence in the current study's cohort aligns reasonably with typical RPD prevalence in each AMD stage, and because the association between AMD and RPD is both strong and consistent, our interstage CC perfusion findings are likely to be more generalizable than if RPD were excluded. The current study did not interrogate a particular potential cause or effect of CC flow impairment (e.g., RPD versus drusen versus other), but rather global and regional flow impairment at each AMD stage, regardless of causes or manifestations of impairment. A GEE subgroup analysis also demonstrated that exclusion of eyes with RPD from the study cohort resulted in statistical significance findings almost identical to those in Table 3, in full affirmation of the central conclusions of the current study. Likewise, although it has been noted that different stages of neovascularization may be reflected in choriocapillaris flow deficit metrics in fellow eyes with dry AMD,³⁷ any potential influence of fellow eye neovascularization has not been described for the current study's cohort, which in any case had a reasonably tight distribution of neovascularized fellow eyes among early, intermediate, and advanced dry AMD stages.

Study weaknesses included its retrospective character, failure to account for hypertension,³⁰ lack of a control population, and a small sample size for eyes with intermediate dry AMD. As noted in related studies,^{16,17} residual superficial projection artifact may still have some effect on CC perfusion imaging despite the use of projection removal software, which is a challenge of imaging the CC on OCTA. There was also a sex imbalance among eyes in this study, although this has not been identified in the literature as a substantial concern. Areas for future investigation include the deployment of the models resulting from this study for CC flow deficit prediction, increasingly robust and regional histologic characterization of the macular CC, and more granular global macular analysis of CC perfusion in the phenotypically heterogeneous advanced dry AMD stage.

Acknowledgments

The authors thank the Ruikang Wang group for permission to use one of their drusen compensation algorithms for comparative purposes: Choriocapillaris flow deficit quantification (6×6) version 1.0b Copyright 2017–2022 University of Washington. Developed in the Biophotonics and Imaging Laboratory (Ruikang Wang). All rights reserved. The authors also thank Luísa Mendonça for assisting with manuscript finalization.

Supported by the Macula Vision Research Foundation (West Conshohocken, PA, USA), the Massachusetts Lions Clubs (Belmont, MA, USA), the National Institutes of Health (Grant Number 5-R01-EY011289-31), the Air Force Office of Scientific Research (Grant Number FA9550-15-1-0473), the Champalimaud Vision Award (Lisbon, Portugal), the Beckman-Argyros Award in Vision Research (Irvine, CA, USA), an NIH–National Institute of Diabetes and Digestive and Kidney Diseases Medical Student Research Fellowship (Award Number T35DK104689), the National Center for Advancing Translational Sciences of the NIH (Award Number TL1 TR001864), and a Yale School of Medicine Medical Student Fellowship (New Haven, CT, USA).

Disclosure: **P.X. Braun**, None; **N. Mehta**, None; **I. Gendelman**, None; **A.Y. Alibhai**, None; **E.M. Moulton**, None; **Y. Zhao**, None; **A. Ishibazawa**, Topcon Medical Systems, Inc. (S), Nidek Medical Products, Inc. (S); **O. Sorour**, None; **E.K. Konstantinou**, None; **C.R. Baumal**, Genentech (C), Carl Zeiss Meditec, Inc. (S); **A.J. Witkin**, None; **J.G. Fujimoto**, Topcon Medical Systems Inc. (F, C), Optovue, Inc. (C, R, S), Carl Zeiss Meditec, Inc. (R); **J.S. Duker**, Carl Zeiss Meditec, Inc. (F, C), Optovue, Inc. (F, C); **N.K. Waheed**, Topcon Medical Systems, Inc. (F), Nidek Medical Products, Inc. (F, S), Carl Zeiss Meditec, Inc. (F), Optovue, Inc. (C)

References

- Garrity ST, Sarraf D, Freund KB, Sadda SR. Multimodal imaging of nonneovascular age-related macular degeneration. *Invest Ophthalmol Vis Sci*. 2018;59:AMD48–AMD64.
- Miller JW. VEGF: from discovery to therapy: The Champalimaud Award Lecture. *Trans Vis Sci Tech*. 2016;5(2):9.
- Miller JW, Bagheri S, Vavvas DG. Advances in age-related macular degeneration understanding and therapy. *US Ophthalmic Rev*. 2017;10:119–130.

4. Brantley MA Jr, Handa JT. Foreword: dry age-related macular degeneration. *Invest Ophthalmol Vis Sci.* 2018;59:AMDi.
5. Spaide RF, Fujimoto JG, Waheed NK, Sadda SR, Staurengi G. Optical coherence tomography angiography. *Prog Retin Eye Res.* 2018;64:1-55.
6. Waheed NK, Moulton EM, Fujimoto JG, Rosenfeld PJ. Optical coherence tomography angiography of dry age-related macular degeneration. *Dev Ophthalmol.* 2016;56:91-100.
7. Rosenfeld PJ. Preventing the growth of geographic atrophy: an important therapeutic target in age-related macular degeneration. *Ophthalmology.* 2018;125:794-795.
8. Borrelli E, Uji A, Sarraf D, Sadda SR. Alterations in the choriocapillaris in intermediate age-related macular degeneration. *Invest Ophthalmol Vis Sci.* 2017;58:4792-4798.
9. Seddon JM, McLeod DS, Bhutto IA, et al. Histopathological insights into choroidal vascular loss in clinically documented cases of age-related macular degeneration. *JAMA Ophthalmol.* 2016;134:1272-1280.
10. Moulton EM, Waheed NK, Novais EA, et al. Swept-source optical coherence tomography angiography reveals choriocapillaris alterations in eyes with nascent geographic atrophy and drusen-associated geographic atrophy. *Retina.* 2016;36(Suppl 1):S2-S11.
11. Sohn EH, Flamme-Wiese MJ, Whitmore SS, et al. Choriocapillaris degeneration in geographic atrophy. *Am J Pathol.* 2019;189:1473-1480.
12. Biesemeier A, Taubitz T, Julien S, Yoeruek E, Schraermeyer U. Choriocapillaris breakdown precedes retinal degeneration in age-related macular degeneration. *Neurobiol Aging.* 2014;35:2562-2573.
13. McLeod DS, Grebe R, Bhutto I, Merges C, Baba T, Luty GA. Relationship between RPE and choriocapillaris in age-related macular degeneration. *Invest Ophthalmol Vis Sci.* 2009;50:4982-4991.
14. Mullins RF, Johnson MN, Faidley EA, Skeie JM, Huang J. Choriocapillaris vascular dropout related to density of drusen in human eyes with early age-related macular degeneration. *Invest Ophthalmol Vis Sci.* 2011;52:1606-1612.
15. Choi W, Moulton EM, Waheed NK, et al. Ultrahigh-speed, swept-source optical coherence tomography angiography in non-exudative age-related macular degeneration with geographic atrophy. *Ophthalmology.* 2015;122:2532-2544.
16. Nassisi M, Baghdasaryan E, Borrelli E, Ip M, Sadda SR. Choriocapillaris flow impairment surrounding geographic atrophy correlates with disease progression. *PLoS One.* 2019;14:e0212563.
17. Thulliez M, Zhang Q, Shi Y, et al. Correlations between choriocapillaris flow deficits around geographic atrophy and enlargement rates based on swept-source OCT imaging. *Ophthalmol Retina.* 2019;3:478-488.
18. Spaide RF, Fujimoto JG, Waheed NK. Image artifacts in optical coherence tomography angiography. *Retina.* 2015;35:2163-2180.
19. Nassisi M, Shi Y, Fan W, et al. Choriocapillaris impairment around the atrophic lesions in patients with geographic atrophy: a swept-source optical coherence tomography angiography study. *Br J Ophthalmol.* 2018;103:911-917.
20. Zhang Q, Zheng F, Motulsky EH, et al. A novel strategy for quantifying choriocapillaris flow voids using swept-source OCT angiography. *Invest Ophthalmol Vis Sci.* 2018;59:203-211.
21. Lane M, Moulton EM, Novais EA, et al. Visualizing the choriocapillaris under drusen: comparing 1050-nm swept-source versus 840-nm spectral-domain optical coherence tomography angiography. *Invest Ophthalmol Vis Sci.* 2016;57:OCT585-OCT590.
22. Borrelli E, Shi Y, Uji A, et al. Topographic analysis of the choriocapillaris in intermediate age-related macular degeneration. *Am J Ophthalmol.* 2018;196:34-43.
23. Sacconi R, Corbelli E, Carnevali A, Querques L, Bandello F, Querques G. Optical coherence tomography angiography in geographic atrophy. *Retina.* 2018;38:2350-2355.
24. Sacconi R, Borrelli E, Corbelli E, et al. Quantitative changes in the ageing choriocapillaris as measured with swept source optical coherence tomography angiography. *Br J Ophthalmol.* 2018;103:1320-1326.
25. Nassisi M, Baghdasaryan E, Tepelus T, Asanad S, Borrelli E, Sadda SR. Topographic distribution of choriocapillaris flow deficits in healthy eyes. *PLoS One.* 2018;13:e0207638.
26. Zheng F, Zhang Q, Shi Y, et al. Age-dependent changes in the macular choriocapillaris of normal eyes imaged with swept-source OCT angiography. *Am J Ophthalmol.* 2019;200:110-122.
27. Boston Image Reading Center. Non exudative AMD imaged with SS-OCT. NLM Identifier: NCT036882432018. Available at: <https://ClinicalTrials.gov/show/NCT03688243>. Accessed March 21, 2019.
28. Ying GS, Maguire MG, Glynn R, Rosner B. Tutorial on biostatistics: linear regression analysis of continuous correlated eye data. *Ophthalmic Epidemiol.* 2017;24:130-140.
29. Alten F, Heiduschka P, Clemens CR, Eter N. Exploring choriocapillaris under reticular pseudodrusen using OCT-angiography. *Graefes Arch Clin Exp Ophthalmol.* 2016;254:2165-2173.
30. Spaide RF. Choriocapillaris flow features follow a power law distribution: implications for characterization and mechanisms of disease progression. *Am J Ophthalmol.* 2016;170:58-67.
31. Ramrattan RS, van der Schaft TL, Mooy CM, de Bruijn WC, Mulder PG, de Jong PT. Morphometric analysis of Bruch's membrane, the choriocapillaris, and the choroid in aging. *Invest Ophthalmol Vis Sci.* 1994;35:2857-2864.
32. Fleckenstein M, Mitchell P, Freund KB, et al. The progression of geographic atrophy secondary to age-related macular degeneration. *Ophthalmology.* 2018;125:369-390.
33. Nesper PL, Soetikno BT, Fawzi AA. Choriocapillaris non-perfusion is associated with poor visual acuity in eyes with reticular pseudodrusen. *Am J Ophthalmol.* 2017;174:42-55.
34. Cicinelli MV, Rabiolo A, Marchese A, et al. Choroid morphometric analysis in non-neovascular age-related macular degeneration by means of optical coherence tomography angiography. *Br J Ophthalmol.* 2017;101:1193-1200.
35. Rabiolo A, Sacconi R, Cicinelli MV, Querques L, Bandello F, Querques G. Spotlight on reticular pseudodrusen. *Clin Ophthalmol.* 2017;11:1707-1718.
36. Wightman AJ, Guymer RH. Reticular pseudodrusen: current understanding. *Clin Exp Optom.* 2018;102:455-462.
37. Borrelli E, Souied EH, Freund KB, et al. Reduced choriocapillaris flow in eyes with type 3 neovascularization and age-related macular degeneration. *Retina.* 2018;38:1968-1976.